

## Supplementary Information

### **Nanoplastics affect the inflammatory cytokine release by primary human monocytes and dendritic cells**

Annkatrin Weber<sup>a</sup>, Anja Schwiebs<sup>b</sup>, Helene Solhaug<sup>c</sup>, Jørgen Stenvik<sup>c,d</sup>, Asbjørn M.

Nilsen<sup>c</sup>, Martin Wagner<sup>e</sup>, Borna Relja<sup>f\*</sup> and Heinfried H. Radeke<sup>b\*</sup>

<sup>a</sup> Goethe University, Department of Aquatic Ecotoxicology, Faculty of Biological Sciences, Max-von-Laue-Straße 13, 60438 Frankfurt am Main, Germany

<sup>b</sup> Goethe University Hospital, Institute of General Pharmacology and Toxicology, pharmazentrum frankfurt, Theodor-Stern-Kai 7/75, 60596 Frankfurt am Main, Germany

<sup>c</sup> Norwegian University of Science and Technology, Department of Clinical and Molecular Medicine, Faculty of Medicine and Health Sciences, Erling Skjalgssons gate 1, Trondheim, Norway

<sup>d</sup> Norwegian University of Science and Technology, Centre of Molecular Inflammation Research, Olav Kyrres gate 17, Trondheim, Norway

<sup>e</sup> Norwegian University of Science and Technology, Department of Biology, Høgskoleringen 5, Realfagbygget, 7491 Trondheim, Norway

<sup>f</sup> Otto-von-Guericke University, Department of Radiology and Nuclear Medicine, Experimental Radiology, Leipziger Str. 44, 39120 Magdeburg, Germany

\*Both authors contributed equally to this work.

---

Corresponding author's contact details: Martin Wagner, martin.wagner@ntnu.no

# S1 Supplementary Introduction

## S1.1 Overview of the most important functions of IL-6, TNF, IL-12p70, IL-23 and IL-10 in inflammatory processes

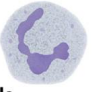
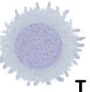

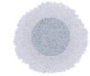

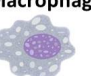



	 <b>Neutrophils</b>	 <b>T cells</b>	 <b>NK cells</b>	 <b>B cells</b>	 <b>Monocytes</b>	 <b>Macrophages</b>	 <b>Dendritic cells (DC)</b>	 <b>Endothelial cells</b>	 <b>Hepatocytes</b>
<b>IL-6</b>	<ul style="list-style-type: none"> <li>➤ (indirect) recruitment of neutrophils to the inflammation site by endothelial cell stimulation [7]</li> </ul>	<ul style="list-style-type: none"> <li>➤ skews T cell differentiation towards pro-inflammatory T cell types (<math>T_H2</math> and <math>T_H17</math>) [7, 8]</li> <li>➤ inhibits immune-suppressing T cells (<math>T_{reg}</math>) [7, 8]</li> <li>➤ reduces T cell apoptosis [7, 8]</li> <li>➤ promotes B cell maturation [9]</li> </ul>			<ul style="list-style-type: none"> <li>➤ Recruitment of mononuclear cells to the inflammation site [7, 8,10]</li> <li>➤ skews monocyte differentiation into macrophages [7]</li> </ul>			<ul style="list-style-type: none"> <li>➤ stimulates endothelial cells to secrete neutrophil-attracting molecules and express adhesion molecules [7, 11]</li> <li>➤ induces acute phase response in hepatocytes [9]</li> <li>➤ regulates IgE-dependent allergy and host defense against staphylococci [12]</li> </ul>	
<b>TNF</b>	<ul style="list-style-type: none"> <li>➤ (indirect) recruitment and activation of neutrophils to the inflammation site by endothelial cell stimulation [13, 14]</li> </ul>	<ul style="list-style-type: none"> <li>➤ early in an inflammation process: induces T cell proliferation [15]</li> <li>➤ later: enhances T cell apoptosis [15]</li> </ul>			<ul style="list-style-type: none"> <li>➤ Indirect recruitment of monocytes to the inflammation site by endothelial cell stimulation [13, 14]</li> <li>➤ enhances DC proliferation, differentiation and migration (both directly and indirectly) [16]</li> </ul>			<ul style="list-style-type: none"> <li>➤ stimulates expression of adhesion molecules on endothelial cells [14]</li> <li>➤ stimulates acute phase-response in hepatocytes [10]</li> <li>➤ can causes tumor growth or necrosis</li> <li>➤ systemic release induces fever, septic shock, organ injuries and cachexia [13]</li> </ul>	
<b>IL-12</b>		<ul style="list-style-type: none"> <li>➤ induces T cell differentiation towards pro-inflammatory T cells (<math>T_H1</math> cells) [17]</li> <li>➤ induces proliferation of NK cells and T cells [17]</li> </ul>						<ul style="list-style-type: none"> <li>➤ may inhibit the growth of several tumor types [17]</li> </ul>	
<b>IL-23</b>		<ul style="list-style-type: none"> <li>➤ induces proliferation and differentiation of pro-inflammatory T cells (<math>T_H17</math> cells) [18]</li> </ul>			<ul style="list-style-type: none"> <li>➤ activates pro-inflammatory cytokine signalling in macrophages [18]</li> <li>➤ stimulates DC antigen-presentation [18]</li> </ul>			<ul style="list-style-type: none"> <li>➤ promotes tumor incidences [17]</li> </ul>	
<b>IL-10</b>	<ul style="list-style-type: none"> <li>➤ inhibits the pro-inflammatory cytokine signalling by neutrophils [19]</li> </ul>	<ul style="list-style-type: none"> <li>➤ inhibits the proliferation and cytokine signalling of pro-inflammatory T cells (<math>T_H1</math> and <math>T_H2</math> cells) [20, 21]</li> <li>➤ inhibits the cytokine signalling of NK cells [19]</li> </ul>			<ul style="list-style-type: none"> <li>➤ suppresses pro-inflammatory functions of monocytes, macrophages and DCs (cytokine signalling, phagocytosis, antigen presentation, migration) [19,20, 21]</li> </ul>				

Fig. S1: Summary of the major functions of IL-6, TNF, IL-12p70, IL-23 and IL-10 in human immune cells ([references S7-20]).

In the human immune system, IL-6 and TNF mostly mediate pro-inflammatory responses while IL-10 acts anti-inflammatory.

Considering the release of IL-6 and TNF, potential downstream effects depend on the cellular and tissue context. Locally high IL-6 and TNF levels can stimulate endothelial cells to recruit neutrophils to the site of inflammation ([S7, 11, 13-14]. In a later stage of the inflammatory process, IL-6 and TNF can also modulate the proliferation of MOs and its differentiation in either macrophages or DCs ([S7-8, 13]). Further, IL-6 can shift the adaptive immune system towards a pro-inflammatory state by enhancing differentiation and proliferation of pro-inflammatory Th17 cells and promoting B cell maturation ([S7-9, 15]). Hence, IL-6 and TNF secretion triggered by exposure to irregular NP may be an initial step towards inflammation.

The release of IL-10, one of the most important anti-inflammatory cytokines, is a typical response to counterbalance inflammation. IL-10 levels usually increase several hours after the release of pro-inflammatory cytokines to prevent an inflammatory overshoot ([S22]). In an early stage, IL-10 suppresses the cytokine production in neutrophils ([S19]). Later on, it inhibits the pro-inflammatory functions of MOs, macrophages and DCs, suppresses pro-inflammatory T cell species and reduces the cytokine release of natural killer cells ([S19-21]).

## **S2 Supplementary Materials & Methods**

### **S2.1 Cell culturing**

#### **S2.1.1 Isolation of PBMCs**

Monocytes (MOs) and monocyte-derived dendritic cells (moDCs) were obtained from peripheral blood mononuclear cells (PBMCs). PBMCs were isolated from human buffy coats by density gradient centrifugation ( $d = 1.077 \text{ g mL}^{-1}$ ) with Histopaque-1077 for moDC experiments (Sigma-Aldrich, Darmstadt, Germany) and Biocoll for MO experiments (Biochrom, Darmstadt, Germany).

For density separation with Histopaque-1077, we prepared a 1:1 mixture of PBS (37 °C, w/o  $\text{Mg}^{2+}$  and  $\text{Ca}^{2+}$ , Gibco Life Technologies/Thermo Fisher Scientific, Darmstadt, Germany) and buffy coat. Several falcon tubes were filled with 12 mL Histopaque-1077 (37 °C) which was overlaid with 32 mL 1:1 PBS-buffy suspension in each falcon. For density separation with Biocoll, we applied the same methodology, but overlaid 25 mL of Biocoll with 25 mL of PBS buffy coat suspension.

All falcons were centrifuged at 400–800 g for 30 min at RT (centrifugal break turned off). PBMCs were isolated from the second topmost cell layer of the gradient, pooled for each buffy coat and washed twice with a threefold volume of PBS (centrifugation in between: 400 g, 10 min, RT). Finally, cells were resuspended in RPMI 1640 medium with supplements.

MO medium included RPMI 1640 + GlutaMAX-I (Gibco Life Technologies/Thermo Fisher Scientific, Darmstadt, Germany) with 2 % (v/v) HEPES (1 M, Sigma-Aldrich, Darmstadt, Germany), 1 % (v/v) Penicillin-Streptomycin (10,000 U  $\text{mL}^{-1}$  penicillin, 10 mg  $\text{mL}^{-1}$  streptomycin, Sigma-Aldrich, Darmstadt, Germany), 1 % Gentamicin Sulfate (50 mg  $\text{mL}^{-1}$ , Lonza, BioWhittaker, Cologne, Germany) and 10 % or 20 % Fetal Bovine Serum (FBS, qualified, heat inactivated, Brazil, Gibco Life Technologies, Darmstadt, Germany).

MoDC medium included RPMI 1640 + GlutaMAX-I with 1 % (v/v) Sodium Pyruvate (100 mM, Gibco Life Technologies, Darmstadt, Germany), 1 % (v/v) Penicillin-Streptomycin (10,000 U  $\text{mL}^{-1}$  penicillin, 10 mg  $\text{mL}^{-1}$  streptomycin, Gibco Life Technologies, Darmstadt, Germany), 0.1 % (v/v)  $\beta$ -mercaptoethanol (50mM, Gibco Life Technologies, Darmstadt, Germany), 1 % (v/v) HEPES (1 M, Sigma-Aldrich, Darmstadt, Germany) and 10 % heat-inactivated human serum. Heat-inactivated

human serum was produced by isolating serum from the topmost layer of the cell gradient, pooling it separately for each buffy coat and heating the serum at 56 °C for at least 30 min. Finally, heat-inactivated serum was centrifuged (1,560 g, 10 min, RT) to remove remaining cell components.

### ***S2.1.2 Separation of monocytes from the PBMC suspension***

Isolated PBMCs were resuspended in MO medium with 20 % FCS. Cells were seeded into 12-well plates (3.8 cm<sup>2</sup>, 7,600,000 cells in 500 µL). After 1 h of incubation at 37 °C and 5 % CO<sub>2</sub>, all non-adherent cells were removed by washing each well three times with MO medium with 10 % FCS. Finally, each well was filled with 600 µL of MO medium with 10 % FCS and cells were directly used for the experiments.

### ***S2.1.3 Differentiation of monocytes into dendritic cells***

Isolated PBMCs were resuspended in moDC medium and seeded into cell culture flasks (175 cm<sup>2</sup>, 200,000,000 PBMCs in 30 mL medium). After 1–2 h of incubation at 37 °C and 5 %, the medium was completely renewed to remove all non-adherent cells. 10 ng mL<sup>-1</sup> human IL-4 (premium-grade, MACS Miltenyi Biotec, Bergisch-Gladbach, Germany), 8 ng mL<sup>-1</sup> recombinant human GM-CSF (PeproTech, Hamburg, Germany) and 3.3 µg mL<sup>-1</sup> ciprofloxacin (hydrochloride, Cayman Chemical, Ann Arbor, MI, US) were added. Cells were incubated for 7 d at 37 °C and 5 % CO<sub>2</sub>. After 4 d, 2/3 of the medium was exchanged and human IL-4, human GM-CSF and ciprofloxacin were added in the same concentrations as before. After 7 d, cells were scraped, pooled for each buffy coat, centrifuged (250 g, 6 min, RT) and resuspended in moDC medium without serum. Finally, moDCs were seeded into 6-well plates (9.6 cm<sup>2</sup>, 750,000 cells in 1 mL of medium), incubated for 1 h at 37 °C and 5 % CO<sub>2</sub> and then directly used for the experiments.

## **S2.2 Preparation of particle stock suspensions**

### **S2.2.1 Solvent removal from PS nanosphere suspensions**

For the removal of the solvent from the PS nanospheres, we centrifuged 1 mL of each suspension, removed the supernatant and washed and centrifuged the spheres (PS<sub>50</sub>, PS<sub>100</sub>, PS<sub>310</sub>) twice with 1 mL of ultrapure water, before resuspending them in 1 mL of physiological saline (154 mmol NaCl). Particle suspensions were centrifuged (Eppendorf, Centrifuge 5424R, Wesseling-Berzdorf, Germany) at 5 °C and 21,130 g for 15 min (PS<sub>310</sub>), 75 min (PS<sub>100</sub>) and 270 min (PS<sub>50</sub>). Centrifugation parameters were determined according to Stokes' Law.

Due to the solvent removal process, 1 µm PS spheres fragmented (Fig. S2) and could not be used for the following cell exposures.

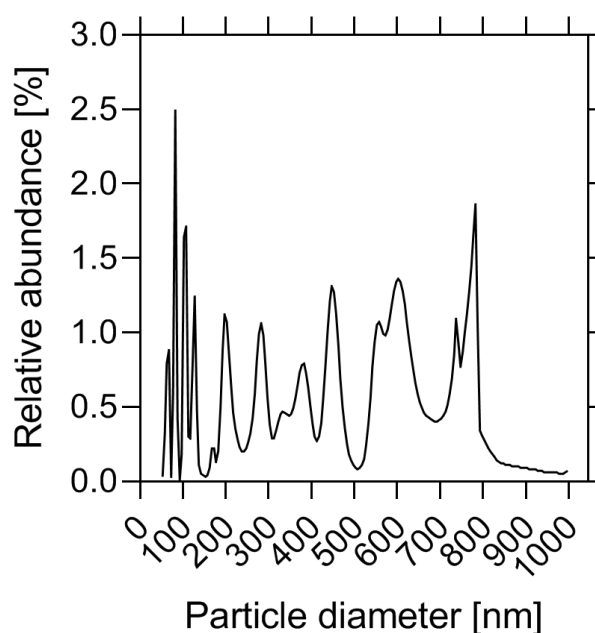


Fig. S2: Particle size distribution (from NTA analysis) of fragmented 1 µm PS spheres after solvent removal process (washing and centrifugation of the spheres).

### **S2.2.2 Production of irregular PMMA and PS particles**

Irregular PMMA and PS particles were prepared using cryomilling: 5 g of plastic pieces (approximately 1×1 cm) were snap frozen in liquid nitrogen for 2 min and ground in a swing mill for 4 min at 30 Hz (MM400, Retsch Technology, Haan, Germany) using a 50 mL milling chamber (01.462.0216, Retsch Technology, Haan,

Germany) and a  $\varnothing$  25 mm stainless steel ball. The cycle of freezing and milling was repeated six times to gain sufficiently small particles. Freezing intervals in-between the grinding is necessary to avoid polymer melting and to facilitate cracking of the polymer structure.

Particle powders were analyzed with scanning electron microscope (SEM, Hitachi, S4500, Krefeld, Germany, Fig. S3). For this, plastic particles were fixed on aluminum discs with coal glue and coated with a gold monolayer (Agar Scientific, Sputter Coater, Stansted, United Kingdom).

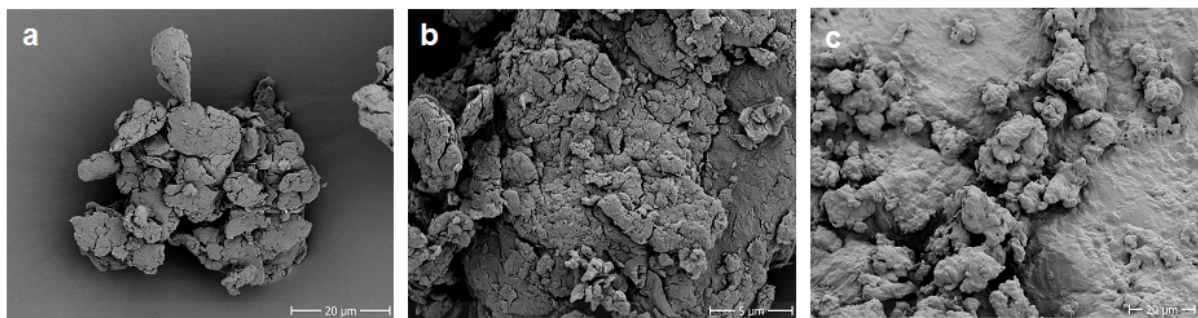


Fig. S3: SEM images of the (a) PS<sub>polyd.</sub>, (b) PMMA<sub>polyd.</sub> and (c) PVC<sub>polyd.</sub> particles prior to the preparation of the stock solutions.

### ***S2.2.3 Preparation of the polydisperse PMMA, PS and PVC stock suspensions***

The preparation of the polydisperse (polyd.) stock suspensions (PMMA<sub>polyd.</sub>, PS<sub>polyd.</sub>, PVC<sub>polyd.</sub>) was performed under sterile conditions except for the lyophilization step. In addition, we rinsed all equipment with ethanol and ultrapure water (sterilized and pre-filtered (0.2  $\mu$ m)) before its use to avoid particle or bacterial contamination. The plastic particles were not sterilized in advance as UV radiation or heating would have changed the polymer properties. Throughout the experiments, we did not observe any bacterial contamination.

To separate the  $\leq 5 \mu$ m particle fraction, 15  $\times$  15–25 mg of plastic powder in 1 mL ultrapure water was transferred into 1.5 mL reaction tubes (Fig. S4). The suspensions were sonicated for 1 h at room temperature (RT). Then, the suspensions were allowed to stand for 12 min (PVC) or 24 min (PS, PMMA) at RT to enable particles  $> 5 \mu$ m to settle. Settling times were determined according to Stokes' Law. The theoretical settling time for PS particles  $> 5 \mu$ m was 114 min. However, as

the particles did not settle but rather adsorbed to the tube surface, the time was reduced to 24 min.

Afterwards, 750  $\mu\text{L}$  supernatant from each reaction tube were pooled and frozen at  $-20\text{ }^{\circ}\text{C}$ . The pooled supernatants were lyophilized to concentrate the particle suspensions. The resulting plastic powders were pooled and resuspended in a total of 1 mL of physiological saline.

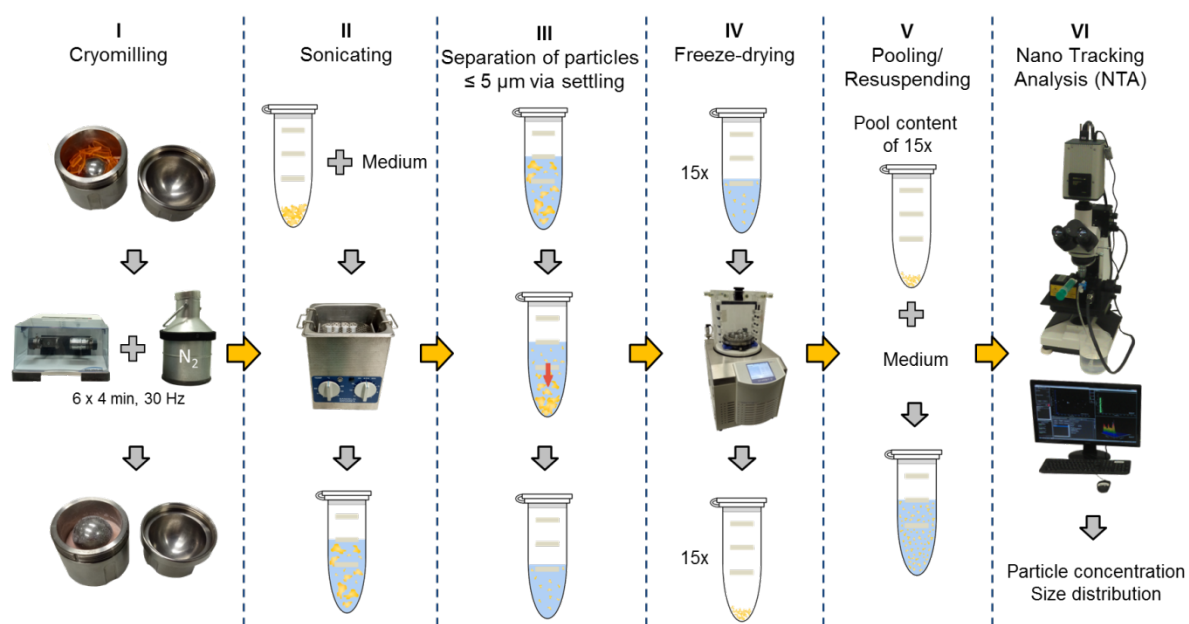


Fig. S4: Preparation of the  $\text{PMMA}_{\text{polyd.}}$ ,  $\text{PS}_{\text{polyd.}}$  and  $\text{PVC}_{\text{polyd.}}$  particle stock suspensions. Step I was not performed with the  $\text{PVC}_{\text{polyd.}}$  particle as those had already been purchased as powder.

### S2.2.4 Preparation of leachates

Polydisperse particle stock suspensions were stored for six weeks at  $5\text{ }^{\circ}\text{C}$  in the dark at RT before the leachates were prepared. 500  $\mu\text{L}$  of each stock suspension were centrifuged (Eppendorf, Centrifuge 5424R, Wesseling-Berzdorf, Germany) three times at  $5\text{ }^{\circ}\text{C}$  for 270 min at 21,130 g to remove all particles  $\geq 50\text{ nm}$ . Between each centrifugation step, we collected and pooled the supernatant to produce  $\text{PMMA}_{\text{leach}}$ ,  $\text{PS}_{\text{leach}}$  and  $\text{PVC}_{\text{leach}}$ .



### **S2.3 ATR-FTIR-spectroscopy**

We confirmed the polymer type of PMMA<sub>polyd.</sub>, PS<sub>polyd.</sub> and PVC<sub>polyd.</sub> by ATR-FTIR spectroscopy (Spectrum 2, Software v10.03.09, Perkin Elmer, Waltham, MA, USA). Spectra were acquired with the range set to 450–4,000 cm<sup>-1</sup> (resolution: 4 cm<sup>-1</sup>, total number of scans: 4, peaks referring to CO<sub>2</sub> and H<sub>2</sub>O were suppressed). The major peaks in the resulting ATR-FTIR spectra were compared to the published spectra in [S1] and [S2]. Results are summarized in chapter S3.1.

### **S2.4 Pyrolysis-GC-MS measurements**

The chemical content of the plastic powders was analyzed qualitatively by pyrolysis-GC-MS (py-GC-MS). 100–300 mg of PMMA, PS and PVC were weighed into a pyrolysis cup each which was sealed with glass fiber stencils. Py-GC-MS analysis was performed with a Multi-Shot Pyrolyzer (EGA/PY 3030D) and an Auto-Shot Sampler (Frontier Laboratories, Saikon, Japan). The pyrolyzer was attached to an Agilent 7890B gas chromatograph (Agilent Technologies, Santa Clara, CA, USA) equipped with an Ultra ALLOY UA-5(MS/HT) metal capillary separation column (Frontier Laboratories, Saikon, Japan, column dimensions: 30 m length, 0.25 mm inner diameter and 0.25 μm film thickness). Chromatographic separation was performed by heating the sample to 280 °C for 5 min. Thermodesorption products were detected with an Agilent 5977B Mass Selective Detector (Agilent Technologies, Santa Clara, CA, USA) in the scheduled selected ion monitoring (SIM) mode for 30 min.

The chromatograms and mass spectra were analyzed with the Agilent MassHunter Workstation Software (version B.05.00, Agilent Technologies, Santa Clara, CA, USA) using Chromatogram Deconvolution. Only peaks with an absolute height of 2 % of the highest peak and with a relative height of at least 5,000 counts were considered. In addition, we chose following settings for peak determination: RT window size factor: 100; peak filter: excluded m/z: 28; extraction window: left m/z delta = 0.3 and right m/z delta = 0.7. The mass spectra were compared to the NIST 2011 Mass Spectral Library (National Institute of Standards and Technology, Gaithersburg, MD, USA). Results are summarized in chapter S3.2.

## ***S2.5 Particle concentrations and size distributions (nanoparticle tracking analysis)***

Concentration and size distribution of the suspended particles were determined by nanoparticle tracking analysis (NTA) with a NanoSight LM10 (Malvern Panalytical, Almelo/Malvern, Netherlands/United Kingdom). We determined particle concentrations and size distributions in the nanosphere (PS<sub>50</sub>, PS<sub>100</sub>, PS<sub>310</sub>) and the polydisperse particle stock suspensions (PMMA<sub>polyd.</sub>, PS<sub>polyd.</sub>, PVC<sub>polyd.</sub>). Due to highly variable concentrations, suspensions were diluted in ultrapure water before NTA (see Tab. S1 for dilution factors and measurement parameters). For each dilution, we prepared a corresponding dilution of the particle-free control with the same dilution factor to obtain comparable control measurements. For the dilution of the PS<sub>polyd.</sub> suspension, a corresponding control dilution of the “PS<sub>polyd.</sub> control” (physiological saline + 1:10,000 Tween<sup>®</sup> 20 (Sigma-Aldrich, Darmstadt, Germany)) was produced (Tab. S1). We prepared three replicates per dilution for each suspension with up to three repeated measurements each. Video capture time was set to 60 s. Video captures were repeated and capture time was prolonged to 120 s in case videos contained < 200 valid particle counts.

Based on the NTA results, particle concentrations in the stock suspensions were blank-corrected by subtracting the particle concentration in the corresponding particle-free control. Then, all suspensions were adjusted to a concentration of 10<sup>10</sup> particles mL<sup>-1</sup> by dilution with physiological saline. The PS<sub>polyd.</sub> control was diluted with physiological saline in the same way as the PS<sub>polyd.</sub> suspension to reduce the Tween<sup>®</sup> 20 content to a corresponding level (Tween<sup>®</sup> 20 content in the final stock solutions: 1:13,350).

We also measured particle concentrations and size distributions in the leachates (PMMA<sub>leach</sub>, PS<sub>leach</sub>, PVC<sub>leach</sub>) to account for remaining particles which had not been removed by centrifugation (see S2.2.4). The NTA was performed in the same way as described above, except that we performed only two replicates with two repeated measurements each (Tab. S1).

Results from NTA measurements are summarized in chapter S3.3.

Tab. S1: Details on nanoparticle tracking analysis for the particle stock suspensions.

Suspension	Dilution factor	Replicates/ Pseudo- replicates	Camera Level	Temperature	Measurement Time	Detection Threshold	Blur	Jump Distance	Min. Track Length
PS <sub>50</sub>	1:1,000,000	3/3	16	37 °C	60 s	10	5x5	12	10
Control for PS <sub>50</sub>	1:1,000,000	3/1	16	37 °C	60 s	10	5x5	12	10
PS <sub>100</sub>	1:300,000	3/3	11	37 °C	60 s	10	5x5	12	10
Control for PS <sub>100</sub>	1:300,000	3/1	11	37 °C	60 s	10	5x5	12	10
PS <sub>310</sub>	1:10,000	3/3	6	37 °C	60 s	10	5x5	12	10
Control for PS <sub>310</sub>	1:10,000	3/1	6	37 °C	60 s	10	5x5	12	10
PMMA <sub>polyd.</sub>	1:200	3/3	6	37 °C	120 s	10	5x5	12	10
Control for PMMA <sub>polyd.</sub>	1:200	3/1	6	37 °C	120 s	10	5x5	12	10
PS <sub>polyd.</sub>	1:100	3/3	6	37 °C	120 s	10	5x5	12	10
Control for PS <sub>polyd.</sub>	1:100	3/1	6	37 °C	60 s	10	5x5	12	10
(1:10,000 Tween 20)									
PVC <sub>polyd.</sub>	1:2,000	3/3	6	37 °C	120 s	10	5x5	12	10
Control for PVC <sub>polyd.</sub>	1:2,000	3/1	6	37 °C	120 s	10	5x5	12	10
PMMA <sub>leach</sub>	1:20	2/2	11	37 °C	120 s	10	5x5	12	10
Control for PMMA <sub>leach</sub>	1:20	2/2	11	37 °C	120 s	10	5x5	12	10
PS <sub>leach</sub>	1:20	2/2	11	37 °C	120 s	10	5x5	12	10
Control for PS <sub>leach</sub>	1:20	2/2	11	37 °C	120 s	10	5x5	12	10
(1:13,350 Tween 20)									
PVC <sub>leach</sub>	1:100	2/2	11	37 °C	120 s	10	5x5	12	10
Control for PVC <sub>leach</sub>	1:100	2/2	11	37 °C	120 s	10	5x5	12	10

Based on the results of the NTA, we used numerical concentrations (particles mL<sup>-1</sup> translated to particle cell<sup>-1</sup>) in our experiments. We also translated the NTA results into other dose metrics to enable comparison with literature data. To do so, we assumed that each size bin from the NTA represents spherical particles of that diameter and used the densities of the three polymers (PS = 1.05 g cm<sup>-3</sup>, PMMA =

1.18 g cm<sup>-3</sup>, PVC = 1.3 g cm<sup>-3</sup>) to derive their mass, volume and surface area (Tab. S2).

Tab. S2: Different dose metrics for the nanoplastics used in this study.

Empirical concentration		Estimated concentrations		
Numerical (particles mL <sup>-1</sup> )	NP type	Mass-based (µg mL <sup>-1</sup> )	Volumetric (mm <sup>3</sup> mL <sup>-1</sup> )	Surface area (mm <sup>2</sup> mL <sup>-1</sup> )
4.54 × 10 <sup>8</sup> (300 particles cell <sup>-1</sup> , experiments with MOs)	PS <sub>polyd.</sub>	4.218	4.02 × 10 <sup>-3</sup>	63.93
	PMMA <sub>polyd.</sub>	4.817	4.08 × 10 <sup>-3</sup>	78.74
	PVC <sub>polyd.</sub>	7.130	5.48 × 10 <sup>-3</sup>	94.26
	PS <sub>50</sub>	0.031	2.98 × 10 <sup>-5</sup>	3.58
	PS <sub>100</sub>	0.251	2.39 × 10 <sup>-4</sup>	14.33
	PS <sub>310</sub>	7.469	7.11 × 10 <sup>-3</sup>	137.67
7.5 × 10 <sup>7</sup> (100 particles cell <sup>-1</sup> , experiments with moDCs)	PS <sub>polyd.</sub>	0.694	6.61 × 10 <sup>-4</sup>	10.52
	PMMA <sub>polyd.</sub>	0.792	6.71 × 10 <sup>-4</sup>	12.95
	PVC <sub>polyd.</sub>	1.173	9.02 × 10 <sup>-4</sup>	15.50
	PS <sub>50</sub>	0.005	4.91 × 10 <sup>-6</sup>	0.59
	PS <sub>100</sub>	0.041	3.93 × 10 <sup>-5</sup>	2.36
	PS <sub>310</sub>	1.228	1.17 × 10 <sup>-3</sup>	22.64

## S2.6 Exposure of moDCs and MOs to plastic particles

Both MOs and moDCs were exposed separately to all eleven particle stock suspensions for 18 h at 37 °C and 5 % CO<sub>2</sub>. Cells were exposed both in absence and in presence of 10 µg mL<sup>-1</sup> (MOs) or 1 µg mL<sup>-1</sup> (moDCs) lipopolysaccharide (LPS, *E. coli* 0127: B8, Sigma Aldrich, Darmstadt, Germany).

MoDCs were treated with 7.5 µL stock suspension well<sup>-1</sup> (100 particles cell<sup>-1</sup>, 7.5 × 10<sup>7</sup> particles mL<sup>-1</sup>). MOs were exposed to 22.8 µL stock suspensions. In contrast to moDCs, the particle:cell ratio was determined after particle exposure by scraping cells and determining the concentrations of adherent MOs in the control wells. In average, each well (500 µL) contained 866,000 ± 318,000 (SD) adherent cells resulting in an exposure ratio of 295 (~300) particles cell<sup>-1</sup> (4.56 × 10<sup>8</sup> particles mL<sup>-1</sup>).

After the exposure, cells were scraped, and cell suspensions were transferred into pre-cooled 1.5 mL reagent tubes. After centrifugation (13,680 g, 6–10 min, 5 °C), supernatants were directly frozen at -80 °C until being analyzed. Procedure was repeated with five buffy coats for moDCs and six buffy coats for MOs.

Moreover, we tested concentration-dependent effects of NP on cytokine signaling by exposing MOs from three buffy coats to PVC<sub>polyd.</sub> at a ratio of approximately 30

(2.3  $\mu\text{L}$  stock suspension), 75 (5.7  $\mu\text{L}$ ), 150 (11.4  $\mu\text{L}$ ) and 300 (22.8  $\mu\text{L}$ ) particles  $\text{cell}^{-1}$ . In each treatment, the volume of the added suspension was kept constant at 22.8  $\mu\text{m}$  by adding the appropriate volume of control suspension.

Cytokine concentrations were analyzed in the supernatants with ELISA assays (R&D Systems, Bio-Techne, Wiesbaden-Nordenstadt, Germany) according to the manufacturer's instructions. We determined IL-6, TNF and IL-10 levels for both MOs and moDCs and IL-12p70 and IL-23 levels for moDCs only. Cytokine concentrations in the supernatants of the MOs and moDCs were determined once or twice for each treatment group.

### ***S2.7 Surface markers of exposed MOs and moDCs***

For moDC surface marker staining, we transferred 1,000,000 moDCs obtained from one buffy coat in 1 mL medium in FACS tubes, centrifuged them (293 g, 2 min, 4 °C) and replaced the supernatant with 500  $\mu\text{L}$  FACS buffer (0.5 % (m/v) BSA and 2 mM EDTA in PBS without  $\text{CaCl}_2$ ). After centrifugation and removal of the FACS buffer, 100  $\mu\text{L}$  FACS block (0.5 % (v/v) of Fc Block in FACS buffer, Human BD Fc Block, BD Biosciences, Heidelberg, Germany) was added for 5 min at RT. Afterwards, cells were washed once with FACS buffer and then treated with 80  $\mu\text{L}$  antibody solution for 30-45 min at RT in the dark. The antibody solutions were prepared according to manufacturer's instructions. We stained moDCs with DCIR (Alexa Fluor 647 Mouse anti-human Clec4A (CD367), catalog no.: 558220), CD11b/Mac-1 (PE-Cy 7 Mouse Anti-Human CD11b/Mac-1, catalog no.: 561685), CD11c (APC Mouse Anti-human CD11c, catalog no.: 559877), MHC2/HLA-DR (PE-Cy 5 Mouse Anti-Human HLA-DR, catalog no.: 562007) and CD83 (PE Mouse Anti-Human CD83, catalog no.: 556855) antibodies from BD Biosciences (Heidelberg, Germany). Cells were treated both separately with each antibody as well as in mixture (mixture 1: DCIR, CD11b/Mac-1, MHC2/HLA-DR, CD83; mixture 2: CD11c, CD11b/Mac-1, MHC2/HLA-DR, CD83). Finally, cells were washed twice with FACS buffer, resuspended in cell fixation buffer (FACS buffer+1 % (m/v) paraformaldehyde) and stored overnight at 4 °C in the dark.

For MO surface marker staining, we prepared adherent MOs from three buffy coats as described in S2.1.2. Adherent cells were scraped and transferred to FACS tubes. After centrifugation (270 g, 5 min, RT), cells were washed twice with FACS buffer and resuspended in 200  $\mu\text{L}$  FACS buffer. We added 5  $\mu\text{L}$  of CD14 (PE anti-human CD14

Antibody, catalog. no: 301806, Biolegend, Koblenz, Germany) and CD16 (Alexa Fluor 647 Mouse Anti-Human CD16, catalog no.: 557710, BD Biosciences, Heidelberg, Germany) antibody and incubated the suspension for 15 min at RT in the dark. Finally, cells were washed with FACS-buffer once and directly analyzed.

Percentage of cells with the corresponding surface markers were determined by FACS measurements (FACS Canto II, BD Biosciences, Heidelberg, Germany). Percentages for MOs with CD14 and/or CD16 surface markers were calculated as mean from the three analyzed buffy coats. Results are summarized in chapter S3.4.

### ***S2.8 Interaction of moDCs with polydisperse PMMA particles and 310 nm PS nanospheres***

We analyzed cell-particle interactions of moDCs with PMMA<sub>polyd.</sub> (green fluorescent) and PS<sub>310</sub> (red fluorescent) particles using confocal laser scan microscopy. 250,000 moDCs (in serum-free medium) were seeded into uncoated 8-well  $\mu$ -slides (Ibidi, Martinsried, Germany). Cells were exposed to particles as described in S2.6. Then, cells were washed twice with 300  $\mu$ L of PBS and incubated with 3.7 % formaldehyde (AppliChem, Darmstadt, Germany) for 10 min at RT. After washing cells twice with PBS, cells were incubated with 300  $\mu$ L Triton X-100 (Sigma-Aldrich, Darmstadt, Germany, 0.5 % in PBS) for 5 min. Cells were washed twice with PBS again and exposed to 300  $\mu$ L of 5 % milk (skim milk powder (Sigma-Aldrich, Darmstadt, Germany) in TBST (0.1 % (m/v) Tris ultrapure (AppliChem, Darmstadt, Germany) in PBS and 0.1 % Tween<sup>®</sup> 20 (Sigma-Aldrich, Darmstadt, Germany)) for 45–60 min at RT. Cells were washed once with PBS and afterwards incubated with 100  $\mu$ L milk with DAPI (2  $\mu$ g mL<sup>-1</sup>, ER-Tracker<sup>™</sup> Blue-White DPX, product no.: E12353, Invitrogen, Darmstadt, Germany) and (in case of PMMA<sub>polyd.</sub> particles) with Alexa Fluor<sup>™</sup> 568 Phalloidin (2 U mL<sup>-1</sup>, catalog no. A12380, Invitrogen, Darmstadt, Germany). Cells were incubated for 30 min at RT in the dark, washed twice with PBS and stored at 4 °C in PBS in the dark. Confocal laser scan microscopy was performed with a Zeiss LSM510 Meta system equipped with an inverted Observer Z1 microscope and a Plan-Apochromat 63 $\times$ /1.4 oil immersion objective (Carl Zeiss MicroImaging, Göttingen, Germany). The results are summarized in Fig. 1 and Fig. S11.

### **S2.9 Assay on endotoxin contamination on PVC<sub>polyd.</sub> particles**

The assay was generally performed as described earlier [S3]. In short, human embryonic kidney (HEK293) cells were grown to approximately 50 % confluency in 96-well plates. The cells were transfected with an NF- $\kappa$ B inducible reporter plasmid encoding Firefly luciferase and a control plasmid with non-inducible expression of Renilla luciferase. Cells were also transfected with expression plasmids encoding human TLR4, MD2, and CD14, or an empty pcDNA3 vector as a control. After further incubation for 24 h, the cells were treated with PVC<sub>polyd.</sub> particles or PBS control for 24 h. As a positive control for the activation of TLR4 signaling ultrapure LPS (100 ng ml<sup>-1</sup> *Escherichia coli* serotype O111:B4, Invivogen) was added. All treatments/stimuli were done in quadruplicate. After incubation, the cells were lysed with passive lysis buffer (Promega), and the amount of Firefly and Renilla luciferase activity in the cell lysates were determined using specific luciferase substrates (Promega) and a luminescence plate reader (Victor3 1420 Multilabel Counter, Perkin Elmer). The Renilla luciferase was used for normalization, and TLR4 activation was calculated as fold Firefly luciferase (NF- $\kappa$ B) induction by treatment relative to non-treated cells. Results of the endotoxin contamination assay are summarized in chapter S3.6.

## S3 Supplementary results and discussion

### S3.1 Results from ATR-FTIR spectroscopy

Comparison of the ATR-FTIR spectra with literature data [S1, S2] confirmed the three polymer types PMMA, PS and PVC. The largest differences between the literature and own spectra (Fig. S5) were observed for PVC. This may be related to additives, such as dyes or pigments.

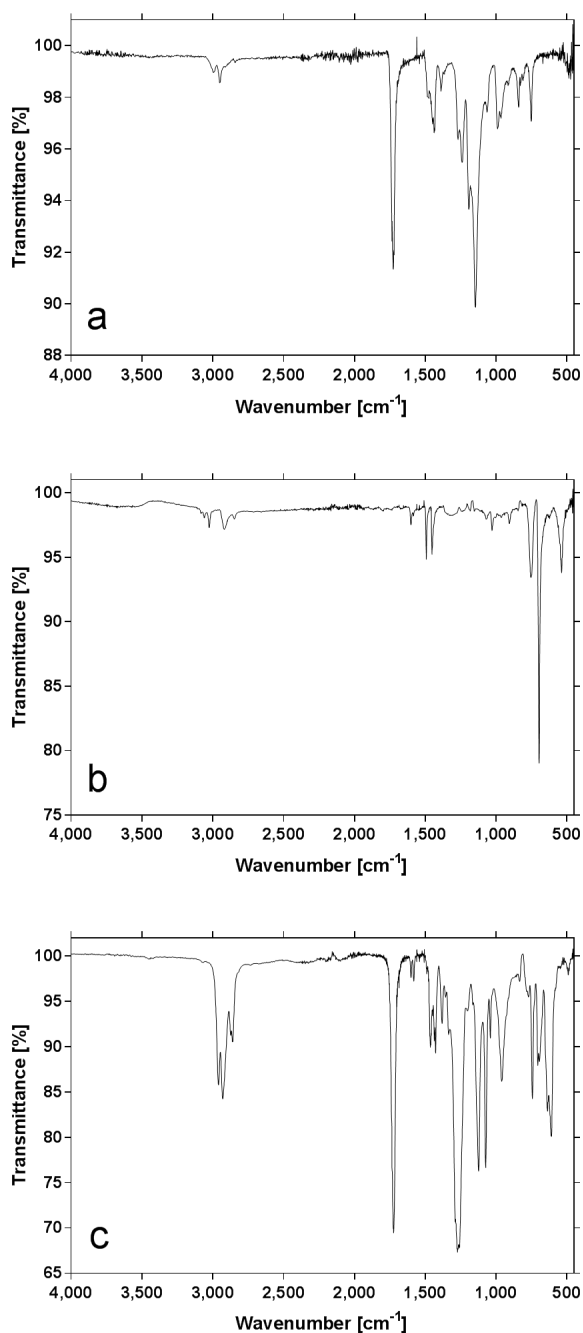


Fig. S5: ATR-FTIR-spectra of the (a) PMMA, (b) PS and (c) PVC plastic powder.



### S3.2 Results from pyrolysis-GC-MS measurements

We detected 10, 2 and 7 peaks in PS, PMMA and PVC, respectively (Tab. S3; Fig. S6). This implies that the polymers contained low numbers of chemicals detectable using py-GC-MS. 1,3-Butadiene,1,4-diphenyl-,(E,E)-, was present in PS<sub>polyd.</sub>. This common fluorophore could origin from the dye. Methyl methacrylate is the monomer of PMMA. The other tentatively identified compounds are not commonly associated with plastics. Importantly, the detected compounds are present in the plastics used in this study. However, that does not necessarily mean that they will leach and be present in the leachates we analyzed *in vitro*.

Tab. S3: Peaks detected in PMMA, PS and PVC and corresponding tentative identification based on the NIST database (highest match scores). Peaks for which NIST did not provide a tentative identification are not included in the table.

	Polymer	Base Peak	RT	Height	Area	Compound name	Score
1	PMMA	136.99	16.168	820,098	6,909,661	Ethanediamide, N-(2-ethoxyphenyl)-N'-(2-ethylphenyl)-	78.21
2	PMMA	69.00	22.526	252,703	4,402,704	Methyl methacrylate	82.37
1	PS	90.99	12.089	21,601	245,656	not identified	none
2	PS	104.01	12.223	14,719	85,223	not identified	none
3	PS	204.02	12.947	6,699	66,710	not identified	none
4	PS	90.99	15.430	622,777	2,067,796	Benzonitrile, m-phenethyl-	57.03
5	PS	90.99	15.856	156,943	1,009,078	1,3-Butadiene, 1,4-diphenyl-, (E,E)-	73.09
6	PS	90.99	15.904	233,782	1,639,405	(2,3-Diphenylcyclopropyl)methyl phenyl sulfoxide, trans-	75.13
7	PS	90.99	15.942	83,831	477,232	(2,3-Diphenylcyclopropyl)methyl phenyl sulfoxide, trans-	59.17
8	PS	90.99	15.983	84,599	781,256	(2,3-Diphenylcyclopropyl)methyl phenyl sulfoxide, trans-	67.09
9	PS	90.99	16.364	14,536	65,237	not identified	none
10	PS	90.99	16.485	6,457	98,021	not identified	none
1	PVC	55.00	9.705	26,713	846,912	1-Decene	79.17
2	PVC	55.00	9.826	10,226	119,675	Cyclopentane, 1,1,3-trimethyl-	79.13
3	PVC	55.00	9.900	9,463	132,868	Cyclopentane, 1,1,3-trimethyl-	78.96
4	PVC	55.00	10.365	27,446	995,255	1-Undecene, 9-methyl-	78.33
5	PVC	55.00	10.483	9,440	118,224	Cyclopentane, 1,1,3-trimethyl-	78.95
6	PVC	55.00	10.555	10,287	136,318	Cyclopentane, 1,1,3-trimethyl-	78.59
7	PVC	55.00	10.997	9,435	342,803	Cyclopentane, 1,1,3-trimethyl-	79.00

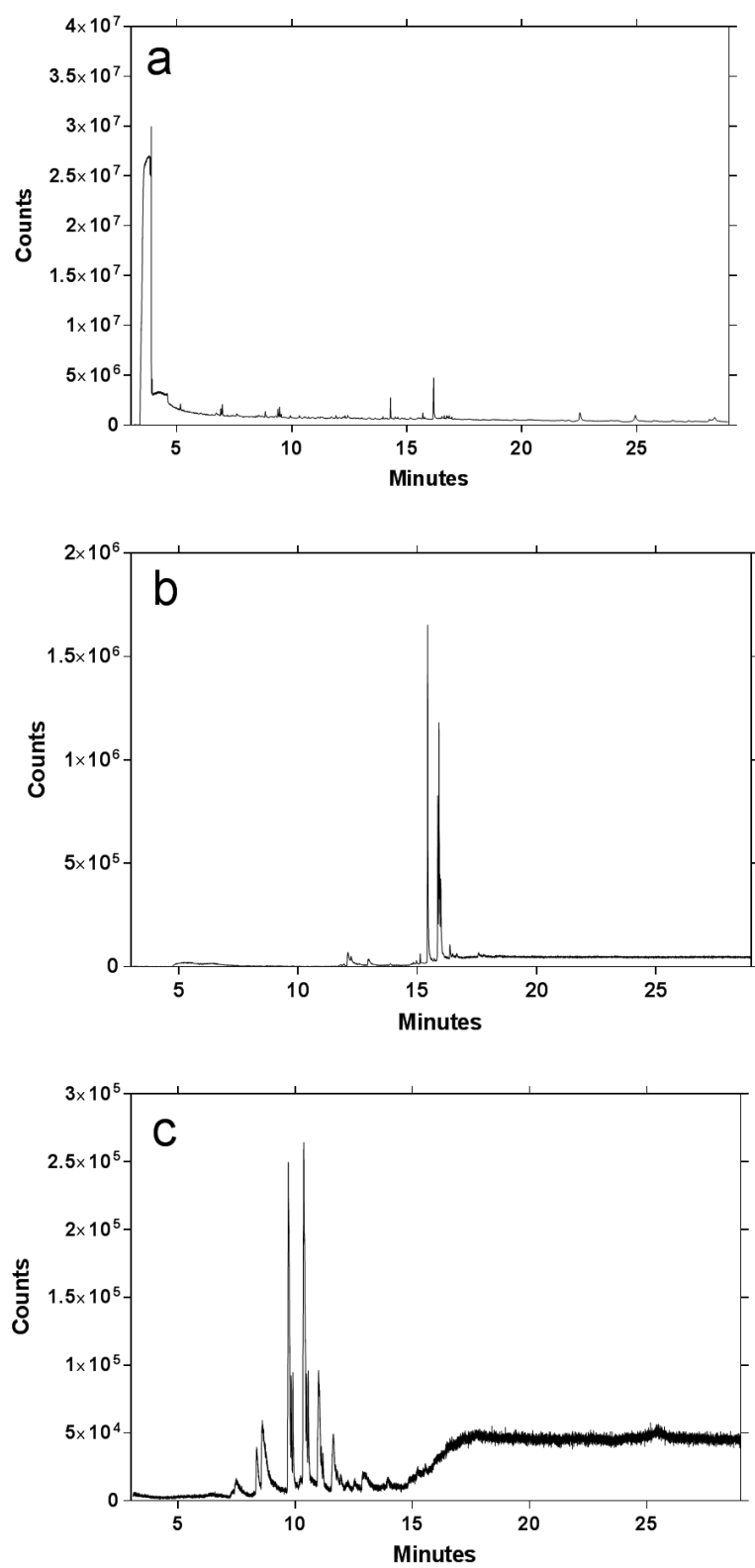


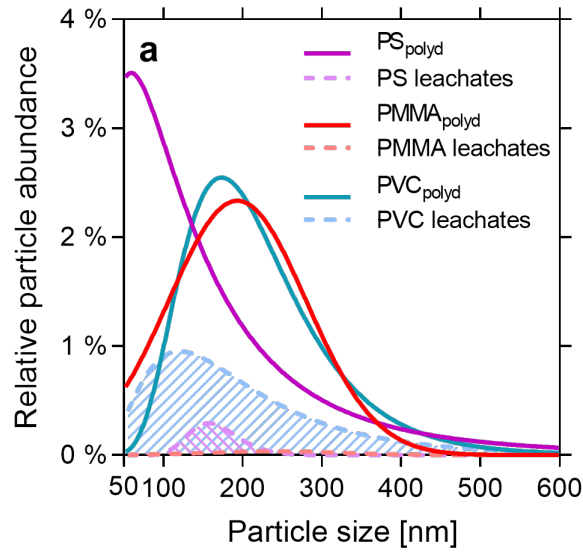
Fig. S6: Total ion current chromatogram of the (a) PMMA, (b) PS and (c) PVC powder in the py-GC-MS.

### **S3.3 Results from nanoparticle tracking analysis**

The particle size distributions from the NTA measurements for particle stock suspensions were fitted with GraphPad Prism (Version 7.04, San Diego, CA) using a Lognormal ( $PS_{\text{polyd.}}$ ,  $PS_{\text{leach}}$ ,  $PVC_{\text{polyd.}}$ ,  $PVC_{\text{leach}}$ ,  $PS_{50}$ ,  $PS_{100}$ ) or Gaussian fit ( $PMMA_{\text{polyd.}}$ ,  $PMMA_{\text{leach}}$ ,  $PS_{310}$ ). Particle size distributions in the PMMA, PS and PVC polydisperse suspension ranged from 50–600 nm (Fig. S7a). The size distributions of the particles in the  $PMMA_{\text{polyd.}}$  and  $PVC_{\text{polyd.}}$  suspensions were comparable with a geometric mean of 193.4 nm ( $PMMA_{\text{polyd.}}$ ) and 203.3 nm ( $PVC_{\text{polyd.}}$ ). For the  $PS_{\text{polyd.}}$  suspensions, we determined a larger fraction of particles < 150 nm (mean: 117 nm). Thus, 50 % of the particles in the  $PMMA_{\text{polyd.}}$  and the  $PVC_{\text{polyd.}}$  suspension were < 210 nm ( $PMMA_{\text{polyd.}}$ ) and < 215 nm ( $PVC_{\text{polyd.}}$ ) compared to < 140 nm in the  $PS_{\text{polyd.}}$  suspension (Fig. S7b).

Throughout the measurements with the  $PS_{\text{polyd.}}$  particles, we observed intensive light scattering due to the highly irregular structure of the particles. Therefore, it is possible that the enhanced abundance of particles < 150 nm in the  $PS_{\text{polyd.}}$  suspension could rather be an artefact induced by the intensive light scattering and the mean size of particles was actually higher than determined with NTA.

In the nanosphere suspensions (Fig. S7c), mean particle sizes were 80.4 nm for  $PS_{50}$ , 104.8 nm for  $PS_{100}$  and 295.5 nm for  $PS_{310}$ . Thus, the particle sizes of  $PS_{100}$  and  $PS_{310}$  were in accordance with the initial particle sizes. For  $PS_{50}$ , instead, the mean size was 60.8 % higher than expected (80.4 nm instead of 50 nm). As 50 nm is the lower detection limit of the NanoSight LM10, visualization of particles with 50 nm by light scattering is challenging and could possibly cause distortions in the particle size calculations. Additionally, particle agglomeration of  $PS_{50}$  spheres could be a cause for the larger mean particle size.



<b>b</b>	PMMA <sub>polyd.</sub>	PS <sub>polyd.</sub>	PVC <sub>polyd.</sub>
99% of particles	< 530 nm	< 600 nm	< 595 nm
95% of particles	< 385 nm	< 430 nm	< 455 nm
90% of particles	< 335 nm	< 335 nm	< 385 nm
75% of particles	< 270 nm	< 215 nm	< 285 nm
50% of particles	< 210 nm	< 140 nm	< 215 nm

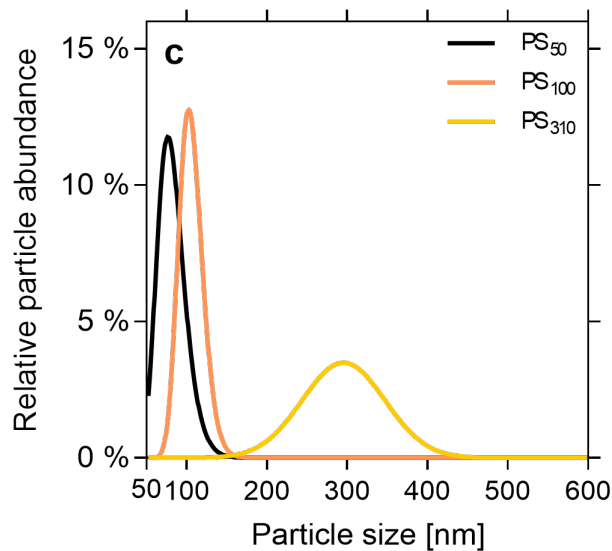


Fig. S7: Size distribution determined by nanoparticle tracking analysis in the (a) PMMA<sub>polyd.</sub>, PS<sub>polyd.</sub> and PVC<sub>polyd.</sub> suspensions and the corresponding leachate controls and in the (c) PS<sub>50</sub>, PS<sub>100</sub> and PS<sub>310</sub> nanosphere suspensions. (b) Details on size distribution in the polydisperse particle stock suspensions.

Particle concentrations in the leachate controls were reduced by 99.2 % (PMMA<sub>leach</sub>), 97.3 % (PS<sub>leach</sub>) and, 80.0 % (PVC<sub>leach</sub>) compared to the corresponding particle stock suspension, Fig. S7a).

### **S3.4 Results from surface marker characterization**

The differentiation of MOs with human IL-4 and human GM-CSF for 7 d produced immature moDCs. As reported earlier [S4], immature moDCs in our study expressed high levels of MHC2/HLA-DR, CD11b/Mac-1 and CD11c (Tab. S4). The high abundance of DCIR as well as the low level of CD83 further emphasized that moDCs had not yet differentiated into mature cells ([S5], [S6]). 91.7 % of the isolated MOs expressed CD14, 0.6 % CD16 and 5.8 % both surface markers. Accordingly, our experiments were mostly performed with MOs (Tab S4).

Tab. S4: Results of surface marker characterization for MOs and moDCs. Percentages indicate the relative proportion of cells possessing the corresponding surface marker, either stained individually or in a mixture. n.a. = not analyzed

		Single staining	Mixed staining 1	Mixed staining 2
	DCIR	76.9 %	98.4 %	n.a.
	CD11b/Mac-1	99.9 %	100 %	100 %
moDCs	CD11c	99.8 %	n.a.	100 %
	MHC2/HLA-DR	99.1 %	99.0 %	99.1 %
	CD83	12.2 %	12.8 %	16.5 %
	CD14	n.a.	91.7 %	n.a.
MOs	CD16	n.a.	0.6 %	n.a.
	CD14 and CD16	n.a.	5.8 %	n.a.

### S3.5 Dose-response relation of MO stimulation with LPS

#### S3.5.1 Absolute cytokine concentrations of the dose-response relation

Tab. S5: Absolute cytokine concentrations in the supernatants of MOs exposure to various doses of LPS.

Cytokine	Donor	Control	10 ng mL <sup>-1</sup> LPS	100 ng mL <sup>-1</sup> LPS	1 µg mL <sup>-1</sup> LPS	10 µg mL <sup>-1</sup> LPS	20 µg mL <sup>-1</sup> LPS	50 µg mL <sup>-1</sup> LPS	100 µg mL <sup>-1</sup> LPS
IL-6 (pg mL <sup>-1</sup> )	Donor 1	25.51	33.94	33.73	33.68	32.35	32.59	40.97	30.23
		22.05	33.07	33.47	33.32	32.60	34.18	32.78	31.21
	Donor 2	24.01	30.07	30.66	31.08	31.65	31.14	30.77	30.70
		23.60	30.42	30.49	30.84	31.13	31.88	31.12	30.48
	Donor 3	30.27	35.49	34.93	47.95	33.05	35.35	33.75	33.57
		29.84	36.61	36.03	31.00	35.56	33.91	33.84	32.10
	Donor 4	32.68	36.58	34.16	33.89	32.79	34.48	30.16	31.02
		25.51	33.94	33.73	33.68	32.35	32.59	40.97	30.23
	Donor 5	0.00	44.01	44.85	45.46	42.75	43.13	43.12	44.17
		0.00	41.18	42.92	41.43	42.64	43.14	41.80	44.72
TNF (pg mL <sup>-1</sup> )	Donor 1	14.05	635.10	761.70	629.91	781.37	764.69	853.73	696.43
		12.13	622.47	634.93	621.33	751.23	742.94	715.01	674.16
	Donor 2	32.28	980.89	1010.80	1371.80	1402.20	1372.60	1402.80	1284.20
		56.46	844.24	1131.30	1374.70	1389.50	1390.40	1360.10	1250.90
	Donor 3	30.88	911.56	837.82	866.63	842.38	888.45	988.39	883.84
		27.77	912.59	836.46	798.10	991.22	881.79	941.52	994.50
	Donor 4	17.55	449.26	497.84	508.11	570.98	573.22	621.50	513.18
		18.19	471.37	504.00	532.37	542.56	618.43	591.19	507.16
	Donor 5	0.00	490.11	577.22	679.06	708.26	944.63	1047.70	984.03
		0.00	525.70	549.89	678.74	715.51	1009.00	1014.60	1013.40

Cytokine	Donor	Control	10 ng mL <sup>-1</sup> LPS	100 ng mL <sup>-1</sup> LPS	1 µg mL <sup>-1</sup> LPS	10 µg mL <sup>-1</sup> LPS	20 µg mL <sup>-1</sup> LPS	50 µg mL <sup>-1</sup> LPS	100 µg mL <sup>-1</sup> LPS
IL-10 (pg mL <sup>-1</sup> )	Donor 1	219.12	5489.70	5763.30	6,784.10	6360.10	6424.50	6080.00	6754.30
		174.49	5890.50	379.60	7107.20	7327.90	6953.80	7172.40	7099.20
	Donor 2	576.59	7695.20	8,626.40	9509.40	10153.00	10120.00	10567.00	10885.00
		1318.00	8135.40	8791.70	9428.30	10383.00	10391.00	10617.00	10775.00
	Donor 3	130.64	3916.10	4141.60	4692.50	5146.70	5121.10	4779.10	4783.80
		113.46	3757.50	3783.50	5054.70	4564.80	4813.00	5187.50	4856.20
	Donor 4	418.90	5189.80	5669.50	7,617.70	8542.60	8652.50	8241.00	9240.00
		449.60	5822.30	6454.40	901.30	8452.00	8843.70	8835.80	9668.10
	Donor 5	0.00	1553.00	1755.10	2116.50	1809.40	1598.90	1397.00	1147.80
		0.00	1692.00	1922.70	2292.20	1694.40	1709.30	1695.70	1224.90

### S3.5.2 Differences in cytokine release to various LPS doses

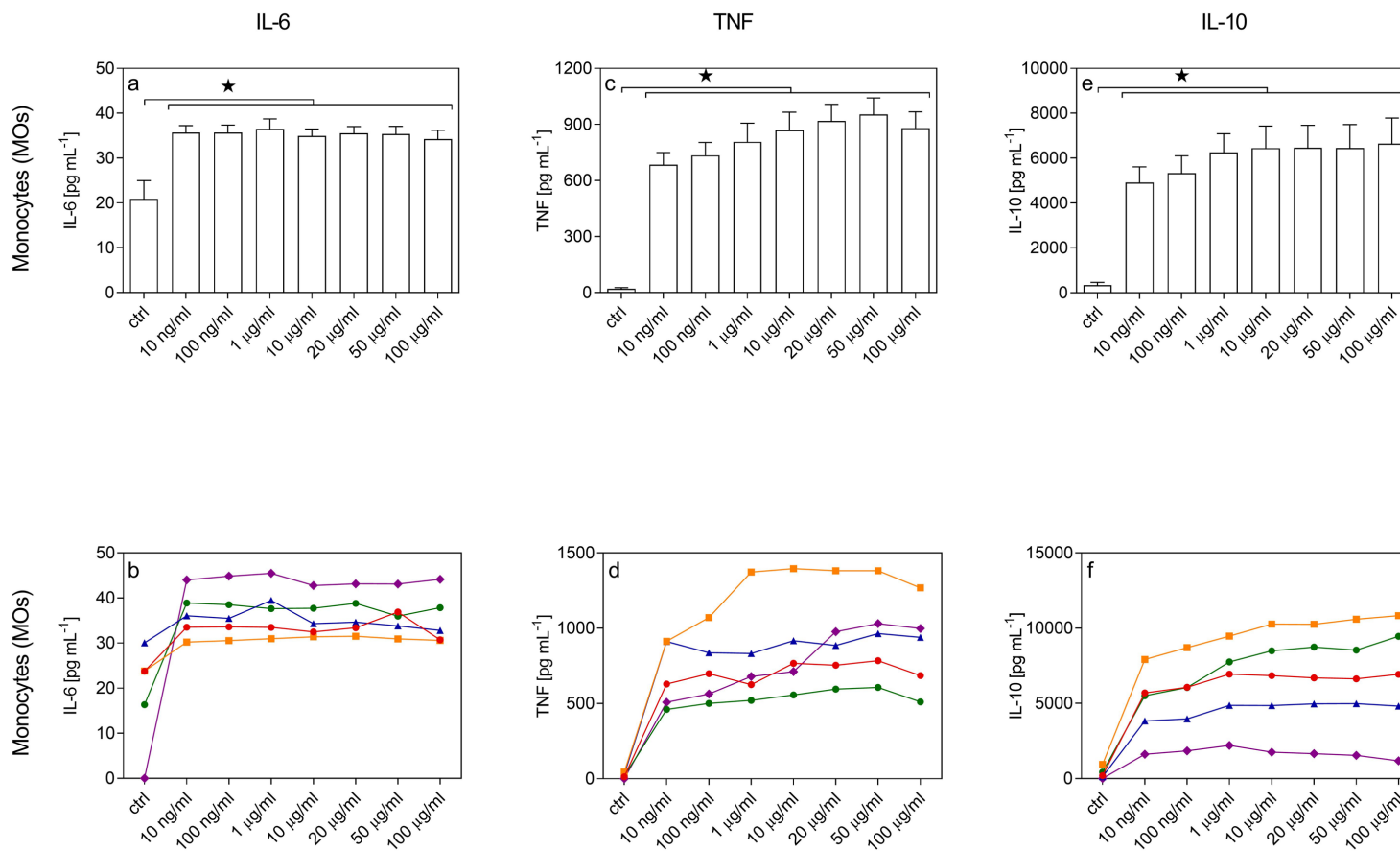


Fig. S8: (a, c, e) Cytokine release of MOs induced by different doses of LPS (10 ng mL<sup>-1</sup> – 100 µg mL<sup>-1</sup>) in MOs from five buffy coats (mean + SEM). Statistical differences were determined using Kruskal Wallis-tests with Dunn's posttest. ★ p < 0.05. (b, d, f) Results from a, c and e presented separately for each of the five buffy coats indicating stimulation response variability between cells from the five buffy coats.



### S3.6 Results for endotoxin contamination on PVC<sub>polyd.</sub> particles

No significant induction of the TLR4-inducible NF- $\kappa$ B reporter was observed during 24 h of treatment with PVC<sub>polyd.</sub> ( $10^6$  and  $10^7$  particles mL<sup>-1</sup>) relative to non-treated controls, while treatment with ultrapure LPS (100 ng mL<sup>-1</sup>) potently activated TLR4 signaling (Fig. S9).

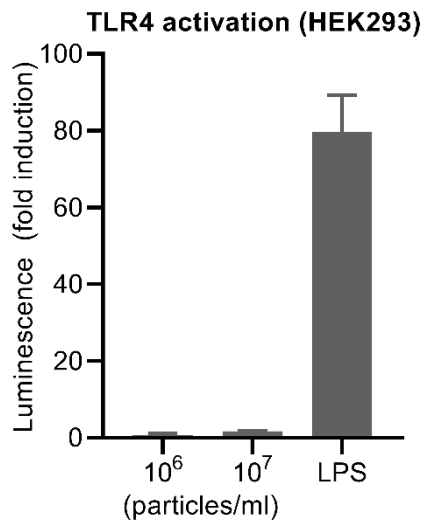


Fig. S9: Investigation of PVC<sub>polyd.</sub> purity using a TLR4-inducible NF- $\kappa$ B reporter assay (HEK293). Cells were transfected with an NF- $\kappa$ B inducible luciferase reporter plasmid and TLR4/MD2/CD14 plasmids, as well as control plasmids, n=4.



### S3.8 Interaction of plastic particles with moDCs

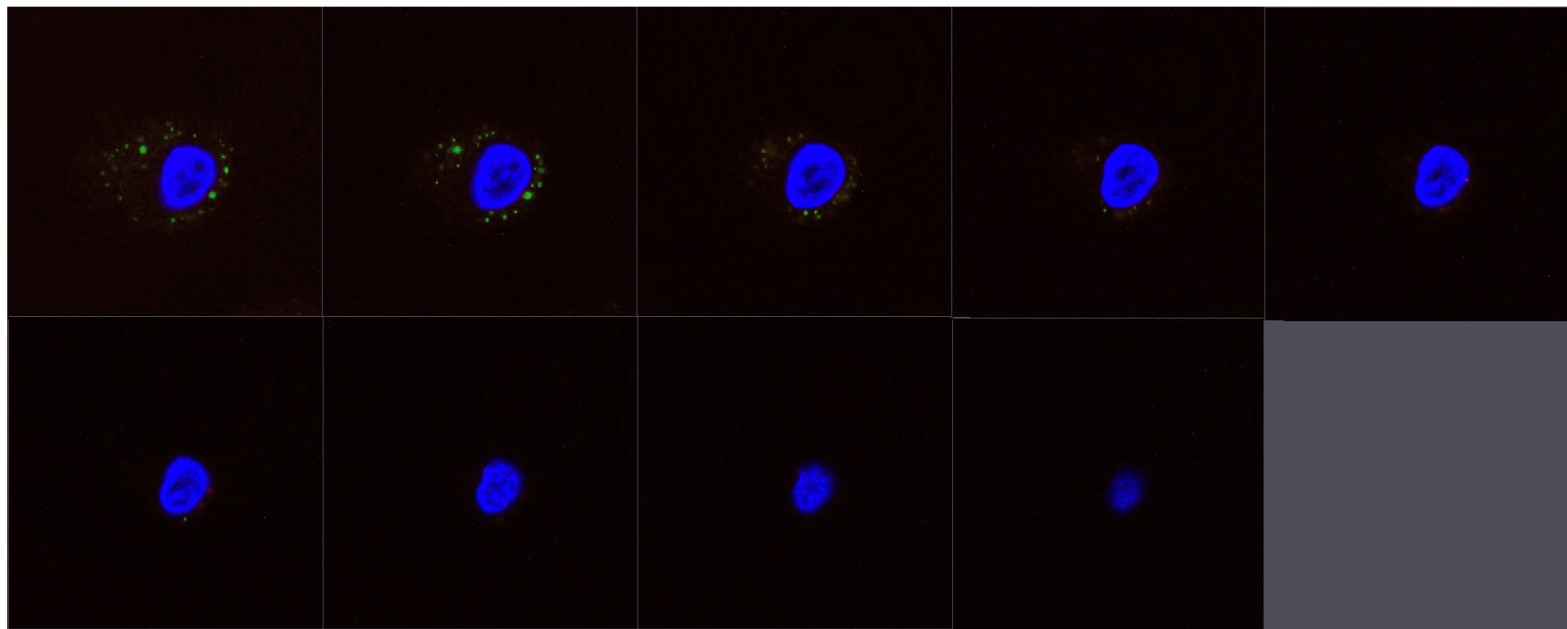


Fig. S11: Interaction of 310 nm PS spheres with moDCs in presence of LPS (Z-stack image series). Images were taken at a 63-fold magnification and a crop-factor of 50. Staining: blue = nuclei (DAPI), green = PS<sub>310</sub>.

### S3.9 Absolute cytokine concentrations in the moDC and MO exposures with plastic particles

Tab. S6: Absolute cytokine concentrations in the supernatants of the moDCs exposure to various plastic particles. In the experiments with moDCs, we detected no IL12p70 in presence or absence of LPS. We detected IL23 only in the presence of LPS. PS<sub>polyd.</sub> control = Tween 20 control

Cytokine	Donor	Control	PS <sub>polyd.</sub> control	PS <sub>polyd.</sub>	PS <sub>leach</sub>	PMMA <sub>polyd.</sub>	PMMA <sub>leach</sub>	PVC <sub>polyd.</sub>	PVC <sub>leach</sub>	PS <sub>50</sub>	PS <sub>100</sub>	PS <sub>310</sub>
IL-6 (pg mL <sup>-1</sup> )	Donor 1	29.79	29.83	37.14	34.68	37.70	32.69	30.32	30.55	35.51	29.57	29.57
	Donor 2	17.99	22.16	25.30	18.29	23.35	21.92	20.95	20.53	21.84	18.42	22.01
	Donor 3	94.07	89.30	113.18	89.79	101.52	77.96	99.75	76.02	90.61	78.28	79.76
	Donor 4	488.02	518.70	1018.92	654.67	789.91	438.20	3866.23	494.99	407.57	393.92	372.31
	Donor 5	229.86	256.40	294.14	207.41	227.31	196.63	5997.03	185.24	205.08	206.56	209.10
TNF (pg mL <sup>-1</sup> )	Donor 1	18.24	16.17	23.46	22.87	20.95	17.22	18.40	16.77	25.73	12.91	13.23
	Donor 2	50.64	44.23	66.07	44.75	72.17	42.76	42.89	38.55	42.69	30.35	45.05
	Donor 3	33.35	27.57	51.81	26.37	54.80	25.45	30.44	30.11	26.94	26.99	24.32
	Donor 4	26.47	35.83	69.12	31.32	38.85	22.25	56.49	25.10	21.61	18.56	20.16
	Donor 5	12.82	20.65	17.85	12.08	12.54	13.53	117.99	12.29	10.56	10.77	11.12
IL-10 (pg mL <sup>-1</sup> )	Donor 1	11.71	9.57	12.24	11.17	9.97	0.74	5.42	7.83	23.10	4.88	4.08
	Donor 4	47.23	57.67	40.84	59.70	52.15	47.84	64.02	56.87	33.85	43.93	45.55
	Donor 5	47.71	37.61	31.29	34.25	41.64	35.86	68.61	37.47	38.15	35.73	39.49
IL-6 (ng mL <sup>-1</sup> )	Donor 1	16.55	17.69	16.79	16.69	15.94	18.31	15.57	15.47	16.02	15.09	15.02
	Donor 2	16.85	20.40	16.54	14.92	16.87	18.09	16.16	17.33	18.03	17.73	17.64
	Donor 3	58.00	60.07	58.45	56.44	51.32	53.77	59.88	61.72	54.49	55.41	49.74
	Donor 4	95.44	108.53	109.17	100.94	93.41	101.84	120.66	102.68	89.52	95.14	92.23
	Donor 5	104.78	105.99	93.07	111.24	105.20	110.73	109.34	105.65	104.80	106.97	98.33

Cytokine	Donor	Control	PS <sub>polyd.</sub> control	PS <sub>polyd.</sub>	PS <sub>leach</sub>	PMMA <sub>polyd.</sub>	PMMA <sub>leach</sub>	PVC <sub>polyd.</sub>	PVC <sub>leach</sub>	PS <sub>50</sub>	PS <sub>100</sub>	PS <sub>310</sub>
TNF (ng mL <sup>-1</sup> )	Donor 1	21.29	25.72	29.71	26.58	25.56	25.99	21.41	20.45	26.21	21.17	23.47
	Donor 2	71.19	63.93	78.25	64.42	75.21	66.81	59.79	53.75	60.09	59.21	63.05
	Donor 3	64.27	66.06	69.48	66.67	65.71	58.41	71.05	64.91	59.85	59.84	51.05
	Donor 4	5.29	4.85	10.92	3.66	7.47	4.85	7.09	10.23	4.47	4.08	3.60
	Donor 5	45.32	44.26	43.84	39.40	44.54	48.13	46.67	41.66	38.36	49.01	41.48
IL-10 (ng mL <sup>-1</sup> )	Donor 1	1.60	1.56	1.77	1.63	1.79	1.46	1.25	1.47	1.52	1.43	1.39
	Donor 2	3.05	2.43	3.42	3.30	3.02	2.93	2.36	2.58	3.08	3.21	2.97
	Donor 3	5.41	5.59	5.05	5.35	5.45	5.46	5.10	5.57	6.28	6.05	4.69
	Donor 4	15.99	14.32	15.70	13.35	14.32	15.64	13.62	15.40	15.54	14.72	13.89
	Donor 5	10.31	10.27	10.60	9.23	9.64	10.60	9.04	9.80	8.60	9.48	8.42
IL-23 (ng mL <sup>-1</sup> )	Donor 1	6.83	7.09	8.15	6.98	6.19	6.49	5.38	5.40	6.88	7.33	7.04
	Donor 2	4.37	4.73	4.69	4.35	2.30	3.13	1.53	2.22	4.44	4.44	5.59
	Donor 3	0.28	0.23	0.26	0.27	0.24	0.28	0.09	0.13	0.43	0.30	0.37
	Donor 4	1.87	2.06	2.00	1.67	1.64	1.69	1.81	1.79	1.64	1.78	1.83
	Donor 5	4.18	4.59	3.86	3.92	3.37	3.37	3.52	3.75	3.63	3.99	3.70

+  
LPS

Tab. S7: Absolute cytokine concentrations in the supernatants of MOs exposure to various plastic particles. PS<sub>polyd.</sub> control = Tween 20 control

Cytokine	Donor	Control	PS <sub>polyd.</sub> control	PS <sub>polyd.</sub>	PS <sub>leach</sub>	PMMA <sub>polyd.</sub>	PMMA <sub>leach</sub>	PVC <sub>polyd.</sub>	PVC <sub>leach</sub>	PS <sub>50</sub>	PS <sub>100</sub>	PS <sub>310</sub>
IL-6 (pg mL <sup>-1</sup> )	Donor 1	9.13	6.54	11.57	11.16	30.32	7.47	392.20	7.98	8.07	5.82	6.42
	Donor 2	18.19	15.95	22.66	30.12	21.32	17.99	401.66	18.06	18.30	21.89	19.33
	Donor 3	53.92	6.87	30.19	12.88	5.92	50.35	378.64	128.73	7.26	15.44	8.05
	Donor 4	28.58	14.23	107.52	66.49	9.35	15.84	458.25	65.48	3.93	6.02	72.72
	Donor 5	17.75	7.52	25.14	7.81	7.85	2.51	471.76	88.71	6.46	5.14	2.99
	Donor 6	6.15	11.61	24.65	5.77	5.25	3.13	445.10	3.82	3.32	4.05	1.95
- LPS TNF (pg mL <sup>-1</sup> )	Donor 1	2.40	1.35	6.06	3.22	4.64	2.37	578.43	2.40	1.55	0.26	0.24
	Donor 2	1.17	1.48	4.49	4.29	1.48	0.61	843.69	1.20	1.60	0.26	1.38
	Donor 3	1.50	0.19	7.93	3.02	0.46	3.84	751.98	23.46	1.23	0.16	0.26
	Donor 4	3.35	2.45	17.85	5.95	2.30	1.78	545.46	6.97	0.79	0.53	3.06
	Donor 5	6.03	4.79	13.88	2.77	4.38	0.08	828.31	10.87	1.06	0.66	0
	Donor 6	2.26	3.19	12.61	1.44	1.22	0.35	409.79	0.06	0.79	1.22	0
IL-10 (pg mL <sup>-1</sup> )	Donor 1	10.66	10.00	5.56	8.44	12.64	4.49	151.82	8.20	22.48	8.44	0.54
	Donor 2	8.02	5.68	1.85	11.08	8.56	11.44	1688.05	13.60	12.40	6.76	7.84
	Donor 3	28.88	17.92	39.58	27.89	66.07	41.39	893.70	45.61	17.80	41.27	48.51
	Donor 4	53.70	9.62	13.43	14.20	36.59	21.74	1027.98	17.06	19.45	33.90	39.56
	Donor 5	4.57	0	0	0	9.24	1.43	456.41	3.90	8.95	5.14	3.14
	Donor 6	14.96	6.38	8.67	6.57	7.05	9.71	262.80	9.14	7.24	10.86	6.47
+ LPS IL-6 (ng mL <sup>-1</sup> )	Donor 1	100.67	91.44	90.71	89.76	97.73	90.10	70.47	105.73	108.58	95.98	100.70
	Donor 2	98.11	94.60	83.17	97.75	104.50	96.45	90.14	110.26	37.49	97.92	90.91
	Donor 3	62.42	63.96	62.36	64.58	69.33	67.82	59.07	55.96	54.10	63.29	65.52

Cytokine	Donor	Control	PS <sub>polyd.</sub> control	PS <sub>polyd.</sub>	PS <sub>leach</sub>	PMMA <sub>polyd.</sub>	PMMA <sub>leach</sub>	PVC <sub>polyd.</sub>	PVC <sub>leach</sub>	PS <sub>50</sub>	PS <sub>100</sub>	PS <sub>310</sub>	
+ LPS (ng mL <sup>-1</sup> )	Donor 4	131.57	101.36	104.74	117.55	118.35	126.31	115.03	121.44	111.44	136.42	136.56	
	Donor 5	84.84	101.65	85.81	63.85	50.61	71.91	81.38	65.88	69.10	82.40	84.54	
	Donor 6	31.00	46.79	35.51	34.73	27.56	34.94	38.21	35.37	11.44	14.46	14.36	
	TNF	Donor 1	3.39	4.35	9.99	5.65	4.02	2.89	2.05	3.69	1.79	2.68	2.28
		Donor 2	6.40	6.44	7.67	7.46	6.23	5.79	7.30	5.70	2.09	5.48	3.91
		Donor 3	6.09	8.44	9.70	10.17	7.73	7.48	6.58	6.68	5.32	6.34	5.21
		Donor 4	3.64	3.75	7.26	4.27	3.68	3.00	3.88	2.68	3.52	2.77	2.78
		Donor 5	9.08	13.49	13.15	7.29	4.51	7.07	7.64	6.53	6.24	8.08	9.02
		Donor 6	2.53	3.10	3.73	2.53	2.19	2.34	2.90	2.22	1.17	1.20	1.40
	IL-10	Donor 1	4.17	4.14	1.85	3.63	4.33	3.27	3.00	3.60	4.82	4.07	4.42
		Donor 2	7.47	6.69	5.04	7.89	7.82	6.70	7.03	6.54	9.18	7.09	9.50
		Donor 3	4.58	2.28	2.20	2.81	3.54	2.32	3.25	2.45	4.25	3.64	4.68
		Donor 4	9.81	5.55	4.36	7.66	7.71	6.78	6.86	6.97	7.56	8.42	9.44
		Donor 5	3.26	2.58	1.99	2.34	1.80	2.29	2.85	2.16	2.48	3.24	2.98
		Donor 6	0.99	1.52	0.50	1.28	0.71	0.85	1.17	1.28	0.05	0.20	0.18

Tab. S8: Absolute cytokine concentrations in the supernatants of MOs exposure to increasing PVC<sub>polyd.</sub> concentrations.

<b>Cytokine</b>	<b>Donor</b>	<b>Control</b>	<b>30 particles cell<sup>-1</sup></b>	<b>75 particles cell<sup>-1</sup></b>	<b>150 particles cell<sup>-1</sup></b>	<b>300 particles cell<sup>-1</sup></b>
IL-6	Donor 1	473.97	554.88	1425.79	3524.77	5688.45
	Donor 2	635.50	615.77	714.03	2930.48	5090.98
	Donor 3	586.85	604.76	610.80	701.33	3921.93
TNF	Donor 1	90.59	129.06	270.32	721.96	2048.42
	Donor 2	35.86	35.65	64.06	135.32	360.75
	Donor 3	211.15	233.48	296.99	510.77	756.46
IL-10	Donor 1	10.42	27.02	65.07	119.08	190.74
	Donor 2	162.77	158.62	236.49	421.63	617.20
	Donor 3	277.16	352.30	404.12	583.25	617.08



### S3.10 Plastic particle effects on the LPS stimulated moDCs and MOs

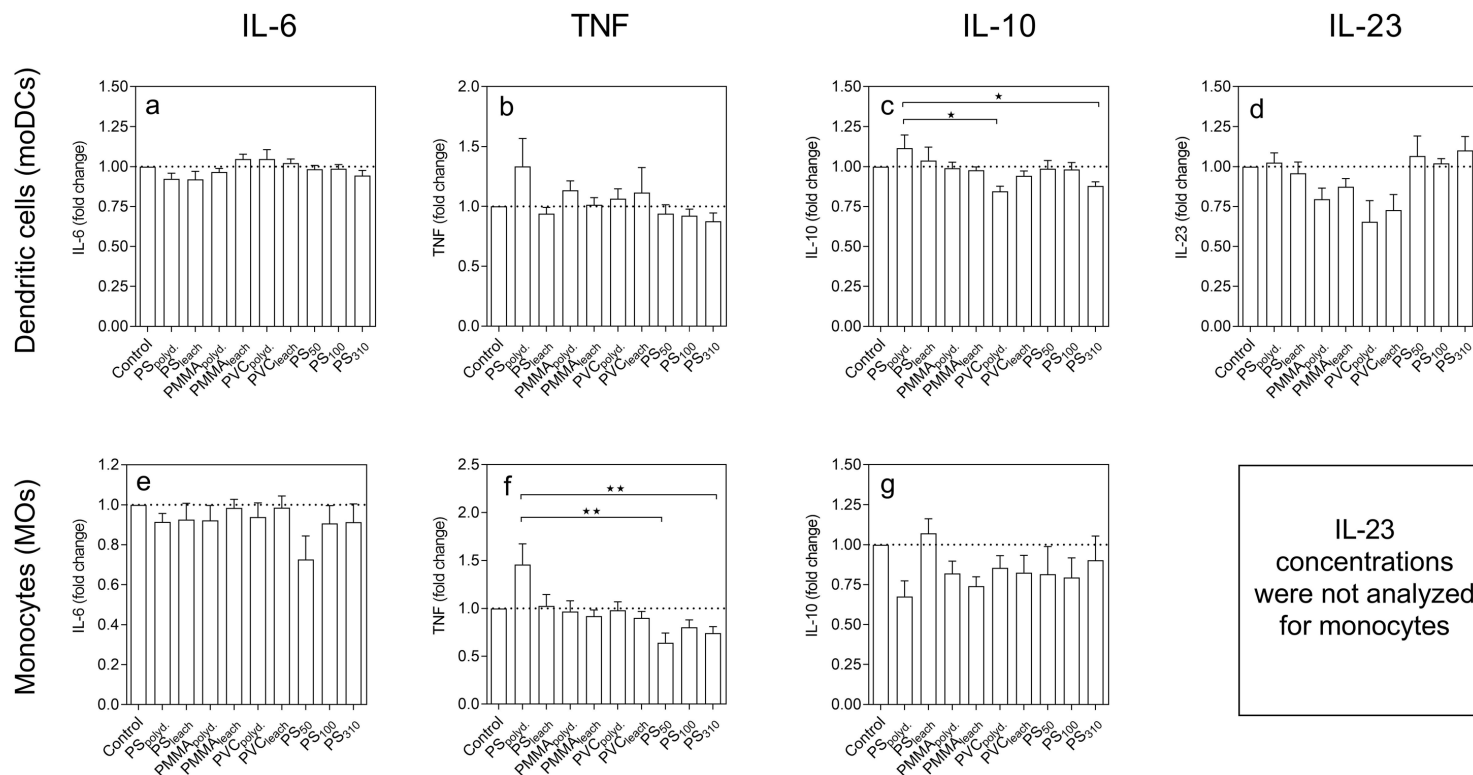


Fig. S12: Effect of plastic particles on the cytokine release of LPS stimulated moDCs (a–d, 50 ng mL<sup>-1</sup> (IL-6, TNF, IL-10), 1 µg mL<sup>-1</sup> (IL-12, IL-23) and MOs (e–g, 10 µg mL<sup>-1</sup>). The release of the cytokines by moDCs (IL-6, TNF, IL-23: n = 5; IL-10: n = 3) and MOs (n = 6) exposed to polydisperse PMMA, PS, PVC (PMMA<sub>polyd.</sub>, PS<sub>polyd.</sub>, PVC<sub>polyd.</sub>), their corresponding leachates (PMMA<sub>leach.</sub>, PS<sub>leach.</sub>, PVC<sub>leach.</sub>) or PS nanospheres (PS<sub>50</sub>, PS<sub>100</sub>, PS<sub>310</sub>) was normalized to the control of the corresponding buffy coat (mean + SEM). Statistical differences were determined using Kruskal-Wallis tests with Dunn’s post test between all exposures and the control, all polydisperse particle exposures and their corresponding leachates as well as between all PS treatments (PS<sub>polyd.</sub>, PS<sub>50</sub>, PS<sub>100</sub>, PS<sub>310</sub>).

★ p < 0.05, ★★ p < 0.01.

### **S3.11 Effects of particle concentration**

Tab. S9: EC<sub>2-fold</sub> results for the release of IL-6, TNF and IL-10 of MOs from three donors exposed to 30–300 PVC<sub>polyd.</sub> particles cell<sup>-1</sup>. EC<sub>2-fold</sub> values estimate the particle concentration which induced 2-fold cytokine concentrations compared to control.

<b>Donor</b>	<b>IL-6</b>	<b>TNF</b>	<b>IL-10</b>
Donor 1	53.2 particles cell <sup>-1</sup>	50.1 particles cell <sup>-1</sup>	10.4 particles cell <sup>-1</sup>
Donor 2	90.5 particles cell <sup>-1</sup>	84.8 particles cell <sup>-1</sup>	108.6 particles cell <sup>-1</sup>
Donor 3	163.9 particles cell <sup>-1</sup>	116.6 particles cell <sup>-1</sup>	141.6 particles cell <sup>-1</sup>

## S4 Supplementary references

- [S1] Jung, M. R., Horgen, F. D., Orski, S. V., Rodriguez, C. V., Beers, K. L., Balazs, G. H., Jones, T. T., Work, T. M., Brignac, K. C., Royer, S. J., Hyrenbach, K. D., Jensen, B. A., Lynch, J. M., 2018. Validation of ATR FT-IR to identify polymers of plastic marine debris, including those ingested by marine organisms. *Marine Pollution Bulletin* 127, 704–716. DOI: 10.1016/j.marpolbul.2017.12.061.
- [S2] Ul-Hamid, A., Soufi, K. Y., Al-Hadhrami, L. M., Shemsi, A. M., 2015. Failure investigation of an underground low voltage XLPE insulated cable. *Anti-Corrosion Methods and Materials* 62(5), 281–287. DOI: 10.1108/ACMM-02-2014-1352.
- [S3] Christiansen, D., Brekke, O. L., Stenvik, J., Lambris, J. D., Espevik, T., Mollnes, T. E., 2012. Differential effect of inhibiting MD-2 and CD14 on LPS- versus whole *E. coli* bacteria-induced cytokine responses in human blood. *Advances in Experimental Medicine and Biology* 946, 237–251. DOI: 10.1007/978-1-4614-0106-3\_14.
- [S4] Sallusto, F., Lanzavecchia, A., 1994. Efficient presentation of soluble antigen by cultured human dendritic cells is maintained by granulocyte/macrophage colony-stimulating factor plus interleukin 4 and downregulated by tumor necrosis factor  $\alpha$ . *Journal of Experimental Medicine* 179(4), 1109–1118. DOI: 10.1084/jem.179.4.1109.
- [S5] Bates, E. E. M., Fournier, N., Garcia, E., Valladeau, J., Durand, I., Pin, J.-J., Zurawski, S. M., Patel, S., Abrams, J. S., Lebecque, S., Garrone, P., Saeland, S., 1999. APCs express DCIR, a novel C-type lectin surface receptor containing an motif immunoreceptor tyrosine-based inhibitory motif. *Journal of Immunology* 163, 1973–1983.
- [S6] Lechmann, M., Berchtold, S., Hauber, J., Steinkasserer, A., 2002. CD83 on dendritic cells: more than just a marker for maturation. *Trends in Immunology* 23(6), 273–275. DOI: 10.1016/S1471-4906(02)02214-7.
- [S7] Scheller, J., Chalaris, A., Schmidt-Arras, D., Rose-John, S., 2011. The pro- and anti-inflammatory properties of the cytokine interleukin-6. *Biochimica et Biophysica Acta* 1813(5), 878–888. DOI: 10.1016/j.bbamcr.2011.01.034.
- [S8] Schaper, F., Rose-John, S., 2015. Interleukin-6: Biology, signaling and strategies of blockade. *Cytokine & Growth Factor Reviews* 26(5), 475–487. DOI: 10.1016/j.cytogfr.2015.07.004.
- [S9] Gruys, E., Toussaint, M. J. M., Niewold, T. A., Koopmans, S. J., 2005. Acute phase reaction and acute phase proteins. *Journal of Zhejiang University-SCIENCE B* 6(11), 1045–1056. DOI: 10.1631/jzus.2005.B1045.
- [S10] Kaplanski, G., Marin, V., Montero-Julian, F., Mantovani, A., Farnarier, C., 2003. IL-6: a regulator of the transition from neutrophil to monocyte recruitment during inflammation. *Trends in Immunology* 24(1), 25–28. DOI: 10.1016/S1471-4906(02)00013-3.
- [S11] Gabay, C., 2006. Interleukin-6 and chronic inflammation. *Arthritis Research & Therapy* 8(2), S3. DOI: 10.1186/ar1917.
- [S12] Puel, A., Casanova, J. L., 2019. The nature of human IL-6. *Journal of Experimental Medicine* 216(9), 1969–1971. DOI: 10.1084/jem.20191002.

- [S13] Tracey, K. J., Cerami, A., 1994. Tumor necrosis factor: A pleiotropic cytokine and therapeutic target. *Annual Review of Medicine* 45, 491–503. DOI: 10.1146/annurev.med.45.1.491.
- [S14] Fiers, W., 1991. Tumor necrosis factor characterization at the molecular, cellular and *in vivo* level. *FEBS Letters* 285(2), 199–212. DOI: 10.1016/0014-5793(91)80803-B.
- [S15] Kollias, G., Kontoyiannis, D., Douni, E., Kassiatis, G., 2002. The role of TNF/TNFR in organ-specific and systemic autoimmunity: Implications for the design of optimized 'anti-TNF' therapies. In: Altman, A. (Ed.), *Signal Transduction Pathways in Autoimmunity. Current Directions in Autoimmunity*. Karger, Basel, 30–50.
- [S16] Tracey, D., Klareskog, L., Sasso, E. H., Salfeld, J. G., Tak, P. P., 2008. Tumor necrosis factor antagonist mechanisms of action: A comprehensive review. *Pharmacology & Therapeutics* 117(2), 244–279. DOI: 10.1016/j.pharmthera.2007.10.001.
- [S17] Xu, M., Mizoguchi, I., Morishima, N., Chiba, Y., Mizuguchi, J., Yoshimoto, T., 2010. Regulation of antitumor immune responses by the IL-12 family cytokines, IL-12, IL-23 and IL-27. *Clinical and Developmental Immunology* 2010, 832454. DOI: 10.1155/2010/832454.
- [S18] Duvallet, E., Semerano, L., Assier, E., Falgarone, G., Boissier, M.-C., 2011. Interleukin-23: A key cytokine in inflammatory diseases. *Annals of Medicine* 43(7), 503–511. DOI: 10.3109/07853890.2011.577093.
- [S19] Opal, S. M., DePalo, V. A., 2000. Anti-inflammatory cytokines. *CHEST* 117(4), 1162–1172. DOI: 10.1378/chest.117.4.1162.
- [S20] Sabat, R., 2013. IL-10 family of cytokines. *Cytokine & Growth Factor Reviews* 21(5), 315–324. DOI: 10.1016/j.cytogfr.2010.11.001.
- [S21] Couper, K. N., Blount, D. G., Riley, E. M., 2008. IL-10: The master regulator of immunity to infection. *Journal of Immunology* 180(9), 5771–5777. DOI: 10.4049/jimmunol.180.9.5771.
- [S22] de Waal Malefyt, R., Abrams, J., Bennett, B., Figdor, C.G., de Vries, J.E., 1991. Interleukin 10(IL-10) inhibits cytokine synthesis by human monocytes: an autoregulatory role of IL-10 produced by monocytes. *J. Exp. Med.* 174(5), 1209-1220. DOI: 10.1084/jem.174.5.1209.